EUROPEAN ORGANIZATION FOR NUCLEAR RESEARCH

CERN–PPE/92–185
October 28, 1992

Search for Anomalous Production of Single–Photon Events in e^+e^- Annihilations at the Z Resonance

L3 Collaboration

Abstract

Using a sample of e^+e^- annihilation events collected at the Z resonance corresponding to an integrated luminosity of 11.2 pb^{-1}, we have searched for γX final states where X represents stable, weakly interacting particles and the energy of the photon is greater than $\frac{1}{2}E_{beam}$. No events were found. The results have been interpreted within a composite Z model and a supergravity model with a light gravitino.

(Submitted to *Physics Letters B*)

1 Introduction

The study of single–photon events—defined as events in which the only detectable final–state particle is a photon—produced in electron–positron annihilations at the Z resonance is sensitive to a variety of new physics processes. New processes contributing to the invisible width Γ_{inv} of the Z may be detected by counting single–photon events which arise from Z decay into stable, weakly interacting particles accompanied by a photon from initial state radiation [1, 2]. For center–of–mass energies near the Z resonance, the energy carried by photons from initial state radiation tends to be a few GeV or less. A number of new physics models, e.g. supersymmetric models and compositeness models, also predict single–photon events in which the photon couples directly to the Z or is produced by a radiative decay in the final state [3, 4, 5, 6, 7]. A specific example is Z $\rightarrow \nu^*\bar{\nu}$, $\nu^* \rightarrow \nu\gamma$, where ν^* is a excited neutrino anticipated in compositeness models [4]. In contrast to Z decay into invisible particles accompanied by a photon from initial state radiation, the energy carried by these photons is typically a sizable fraction ($\sim$0.5 or greater) of the beam energy over a large region of the model parameter space.

In what follows, we report on the search for energetic single–photon events ($E_\gamma > \frac{1}{2}E_{beam}$) in the data collected by L3 at LEP in 1991. As indicated in the preceding paragraph, the results of this search are directly relevant to models that predict single–photon events due to direct coupling to the Z or or due to radiative decay. In particular, we use the search results to strengthen the experimental limits on the electric dipole transition of the Z, which in turn constrains Z compositeness models, and on the gravitino mass for a supergravity model in which the gravitino is assumed to be very light. Limits on neutrino compositeness, derived from an analysis of energetic single–photon events by L3, are published elsewhere [8].

2 The L3 Detector

The L3 detector at LEP is designed to measure the energy and direction of leptons and photons with high precision. A detailed description of the detector and its performance can be found in [9]; here we only outline the features which are relevant to the present analysis.

The detector consists of a central tracking chamber (TEC), a forward–backward tracking chamber (FTC), a high–resolution electromagnetic calorimeter made of about 11000 bismuth germanium oxide (BGO) crystals, a hadron calorimeter (HCAL) with uranium absorber and brass proportional wire chambers, and a high–precision muon spectrometer. A cylindrical array of 30 scintillation counters is installed in the barrel region between the BGO and HCAL. These detectors are located inside a 12–meter solenoid magnet which provides a uniform field of 0.5 T along the beam direction. Forward BGO arrays, on either side of the detector, are used to monitor the luminosity via the detection of small–angle Bhabha events.

The polar angle coverage of the BGO barrel extends from 42.3° to 137.7° while that of the BGO endcaps extends from 11.4° to 35.2° and from 144.8° to 168.6°. The HCAL covers polar angles between 6° and 174°, and the luminosity monitors span the angular region between 1.5° and 4.0° from the beamline. Apart from the region below the minimum detection angle of 1.5°, there is a region between 4° and 6° from the beamline not covered by any detector. In addition, between 6° and 9° the efficiency of the hadron calorimeter for electrons and photons is limited due to the two small lead rings installed in front of it in July 1991 to shield the TEC from the beam halo.

The response of the L3 detector is modeled using the GEANT [10] detector simulation program which includes the effects of energy loss, multiple scattering, and showering in the detector materials and beam pipe. Hadronic showers in the calorimeters are simulated with the GHEISHA [11] program, and the showers due to the natural radioactivity of the uranium are also simulated. In the work described below, Monte Carlo events were passed through the same event reconstruction and analysis programs as the data.

3 Event Selection

Event selection was carried out on the data sample, corresponding to approximately 300K hadronic Z decays, collected by L3 during the 1991 LEP run. The L3 detector triggered on energetic single–photon events using the logical OR combination of the BGO energy triggers, described in detail in [12]. The thresholds of the triggers active in the geometrical acceptance defined by our analysis cuts lay below 10 GeV.

To select energetic single–photon events, allowing for the possibility of an additional soft photon from initial state radiation, we applied the following cuts:

1. At least one BGO cluster with (a) energy greater than $\frac{1}{2}E_{beam}$ and (b) polar angle in the range $20° < \theta < 34.5°$, $44.5° < \theta < 135.5°$, or $145.5° < \theta < 160°$.
2. No more than two BGO clusters in the endcaps and barrel. To be counted, a BGO cluster must contain at least 3 crystals and the most energetic crystal deposit must exceed 100 MeV.
3. The energy of the second most energetic BGO cluster, if present, is less than 1 GeV.
4. The number of TEC tracks is zero.
5. No scintillator counter hits in time with the beam crossing. In applying this cut, we excluded the counters overlapping the energetic BGO cluster because such counters may fire due to shower leakage.
6. The total energy deposited in the HCAL is less than 5 GeV.
7. The total energy deposited in the luminosity monitors is less than 5 GeV.
8. No track reconstructed by the muon chambers and at most one segment of a track found.

9. The transverse shape of the most energetic BGO cluster is consistent with a photon originating from the interaction point.

In addition to the cuts itemized above, we required that all detector subsystems be operational at the time of the event.

Cut 1 defines the fiducial regions in energy and polar angle for our search so as to retain good acceptance for events from the new physics processes of interest while suppressing the background from neutrino pair production accompanied by initial–state radiation and eliminating the background due to QED events, e.g. $e^+e^- \to e^+e^-\gamma$, in which all final–state particles but the photon escape undetected. Cuts 2–8 reject hadronic and charged leptonic decays of the Z, QED events having a topology in which the photon is not the only final–state particle within the acceptance, and beam–gas interactions. Cut 9, aided by Cut 8, eliminates cosmic–induced showers.

No events survive the cuts. The number of events expected from production of neutrino pairs accompanied by a photon from initial state radiation, according to the Standard Model with three neutrino families, is 0.2.

We have studied the efficiency of the selection cuts using Monte Carlo, random trigger events, and large–angle $e^+e^- \to e^+e^-$ events. The trigger efficiency was measured by simulation following a procedure similar to the one we used to measure our trigger efficiency for low–energy single–photon events [13]. The combined selection and trigger efficiency, averaged over the azimuthal angle, is independent of photon energy for the range of interest and varies between 0.84 and 0.92 over the polar angle regions defined in Cut 1. Summed over all center–of-mass energies, the integrated luminosity is 11.2 pb^{-1}, of which 6.7 pb^{-1} was collected at $\sqrt{s} = 91.25$ GeV.

4 Results

4.1 Composite Z

If the Z is assumed to be a bound state of charged constituents, one consequence is an enhancement in the strength of the electric dipole transition ($\mathrm{Z} \to \gamma\mathrm{Z}^*$ where Z^* is virtual) [5], hereafter referred to as EDT. The form factor for this transition, in the case that the initial Z is nearly on–shell, may be parameterized as [14]

$$f \;=\; \beta(\frac{s'}{m_{\mathrm{Z}}^2} - 1)$$

where s′ is the mass–squared of the Z^* and β is the parameter characterizing the strength of this transition. In the Standard Model β is $\mathcal{O}(10^{-5})$, whereas if the Z is composite, β could be several orders of magnitude larger [15]. A previous study of this model taking into account LEP results on the decay $\mathrm{Z} \to \mu^+\mu^-\gamma$ obtained the limit $\beta < 5.9$ [16].

We are interested in the case where EDT makes a contribution to single–photon final states through the Z^* decaying into a neutrino pair. Starting from the Born–level differential cross section for $e^+e^- \to \nu\overline{\nu}\gamma$, events were generated at each of the seven center–of–mass energies for $\beta = 1$. As part of the generation procedure, we included the $\mathcal{O}(\alpha)$ corrections to the Born terms from initial state radiation. The generated events were passed throught the detector simulation program, reconstructed, and subjected to our selection cuts and weighted by the trigger efficiency. The surviving events were then summed over center–of–mass energy.

Figure 1 shows the energy spectra for data and expectations from Monte Carlo for $E_\gamma > 15$ GeV. The plot was obtained by applying the same cuts as those listed in Section 3 except that a cluster energy greater than 15 GeV, rather than $\frac{1}{2}E_{beam}$, was required. The lower limit of 15 GeV is chosen in order to show clearly that the requirement $E_\gamma > \frac{1}{2}E_{beam}$ is appropriate for effectively suppressing Standard Model backgrounds while retaining high acceptance for photons due to EDT. The cross–hatched histogram is the Standard Model expectation ($\beta = 0$) for $e^+e^- \to \nu\overline{\nu}\gamma$ while the sum of the open histogram and the cross–hatched histogram represents the expectation for $\beta = 1$. The contribution expected from the QED processes (shaded histogram) is also shown. The enhancement in the single–photon energy spectrum at high energies from EDT for $\beta = 1$ would be clearly visible.

We have obtained a limit on β as follows. Since the EDT strongly dominates radiative production of neutrino pairs for $E_\gamma > \frac{1}{2}E_{beam}$ and $\beta = \mathcal{O}(1)$, we may parameterize the expected number of events from EDT as $A\beta^2$ where A is the number of events expected at $\beta = 1$. From the Monte Carlo analysis described above, we obtain $A = 5.2$. Based on a study of the uncertainties arising from finite Monte Carlo statistics and systematics in the event selection, trigger efficiency measurement, luminosity calculation, and Monte Carlo event generation, we estimate the fractional uncertainty in expected number of events to be 6%. To arrive at a conservative estimate of the limit on β at the 95% C.L., we incorporate the uncertainty into our procedure by scaling the parameter A downward by 10% ($1.6 \times 6\%$) from 5.2 to 4.7. Given that no events are observed, we finally obtain

$$\beta \ < \ 0.80$$

at the 95% C.L.

4.2 Superlight Gravitino (SLG)

A possible scenario within general supergravity models is that the gravitino, rather than having a mass which is $\mathcal{O}(m_\mathrm{W})$ as in the minimal model, has a mass which is $\mathcal{O}(m_\mathrm{W}^2/m_{Planck})$ [6]. Since the gravitino's coupling to other particles varies as $\sqrt{8\pi G}/m_{\tilde{\mathrm{G}}}$, G being Newton's gravitational constant and $m_{\tilde{\mathrm{G}}}$ the gravitino mass, the reaction

$$\mathrm{Z} \ \to \chi\tilde{\mathrm{G}} \ ; \ \chi \ \to \ \tilde{\mathrm{G}}\gamma$$

where χ is the lightest neutralino, would take place at a significant rate for a sufficiently light gravitino. Furthermore, given that the gravitino is the lightest supersymmetric particle in this scenario and R–parity conservation is assumed, the gravitinos would generally escape undetected, yielding the single–photon event signature.

Events for the process

$$e^+e^- \rightarrow \tilde{G}\tilde{G}\gamma$$

were generated according to the differential cross section (first–order initial–state radiation was included) for several different sets of values for the supersymmetry parameters tanβ, μ, and M and for the gravitino mass $m_{\tilde{G}}$. In the notation used here, M is the Majorana mass term for the winos, μ is the higgsino mass mixing parameter, and tanβ is the ratio of the higgs vacuum expectation values [17]. After detector simulation, the events were reconstructed and passed through our event selection. Figure 2 shows the energy spectra for data and Monte Carlo at $\sqrt{s}$ = 91.25 GeV. The open histogram is the spectrum expected from $e^+e^- \rightarrow \tilde{G}\tilde{G}\gamma$ for tanβ = 2, μ = –100 GeV, M = 30 GeV, and $m_{\tilde{G}}$ = 3×10^{-14} GeV. As in Figure 1, the cross–hatched histogram represents the expected contribution from the radiative production of neutrino pairs, and the shaded histograms the contribution from QED processes. Typical of the SLG scenario, the single–photon energy spectrum expected from $e^+e^- \rightarrow \tilde{G}\tilde{G}\gamma$ extends to high energies.

Given the wide range of allowed values for the parameters tanβ, μ, and M, we set lower limits on $m_{\tilde{G}}$ according to the following method. The cross section renormalization factor due to initial state radiation was determined as a function of $\sqrt{s}$ and the mass of the lightest neutralino. This was incorporated into a program which integrated the product of the Born–level differential cross section, the trigger efficiency, the selection cut efficiency, and the initial state radiation scale factor over photon energy and angle; multiplied the result by the integrated luminosity; and summed over the center–of–mass energies to obtain the expected number of events for the chosen parameter values and gravitino mass. To take into account our uncertainties, we rescaled the expected number of events by 0.9. Finally, the lower limit on $m_{\tilde{G}}$ at 95% C.L. for given choice of SUSY parameters was obtained by varying $m_{\tilde{G}}$ to determine the value for which 3 events would be expected. This method was checked with the results from our analysis of the Monte Carlo samples generated for several specific sets of values for the SUSY parameters and $m_{\tilde{G}}$. The calculation of the cross section assumed that the branching ratio for $\chi \rightarrow \tilde{G}\gamma$ is 1. This assumption is valid for a gluino mass greater than 100 GeV and sfermion masses greater than twice the gluino mass [6]. In the case that the branching ratio is less than 1, our limits must be multiplied by the square root of the branching ratio.

The 95% C.L. lower limits on the gravitino mass as a function of μ for several different choices of M are plotted in Figs. 3. As a function of tanβ, the weakest limits for negative μ are obtained at tanβ = 1, while for positive μ the strongest limits on the gravitino mass are obtained at approximately tanβ = 1. As tanβ is increased while holding M constant, the cross section for $\mu < 0$ increases monotonically while the cross section for $\mu > 0$ decreases nearly monotonically. At small $|\mu|$, the ability to set lower limits on the gravitino mass is diminished because in this region of parameter space the lightest neutralino approaches pure higgsino, which does not couple to the Z and γ. For most of the parameter space bounded by $|\mu| > 50$ GeV and $M < 100$ GeV, the limits shown preclude a gravitino mass less than 10^{-14} GeV and for large regions of the parameter space, the lower limits are substantially stronger.

5 Summary

We have searched for energetic single–photon events ($E_\gamma > \frac{1}{2}E_{beam}$) in the data collected by L3 during the 1991 LEP run. No events were found. This result has been used to extend the experimental limits on the electric dipole transition of the Z, which in turn constrains models of Z compositeness, and on a supergravity model in which the gravitino is assumed to be extremely light. Specifically, we have found that the parameter β, used to characterize the strength of the Z electric dipole transition, is less than 0.80 at the 95% confidence level and that, for a wide region of supersymmetric parameter space, the data rule out the existence of a superlight gravitino with mass less than 1×10^{-14} GeV.

6 Acknowledgments

We wish to express our gratitude to the CERN accelerator divisions for the excellent performance of the LEP machine. We acknowledge the contributions of all the engineers and technicians who have participated in the construction and maintenance of this experiment. Those of us who are not from member states thank CERN for its hospitality and help.

The L3 Collaboration:

O.Adriani,[14] M.Aguilar-Benitez,[23] S.Ahlen,[9] J.Alcaraz,[15] A.Aloisio,[26] G.Alverson,[10] M.G.Alviggi,[26] G.Ambrosi,[31] Q.An,[16] H.Anderhub,[45] A.L.Anderson,[13] V.P.Andreev,[35] T.Angelov,[13] L.Antonov,[39] D.Antreasyan,[7] P.Arce,[23] A.Arefiev,[25] A.Atamanchuk,[35] T.Azemoon,[3] T.Aziz,[8,1] P.V.K.S.Baba,[16] P.Bagnaia,[34] J.A.Bakken,[33] L.Baksay,[41] R.C.Ball,[3] S.Banerjee,[8] J.Bao,[5] R.Barillère,[15] L.Barone,[34] A.Baschirotto,[24] R.Battiston,[31] A.Bay,[17] F.Becattini,[14] U.Becker,[13,45] F.Behner,[45] J.Behrens,[45] S.Beingessner,[4] Gy.L.Bencze,[11] J.Berdugo,[23] P.Berges,[13] B.Bertucci,[31] B.L.Betev,[39,45] M.Biasini,[31] A.Biland,[45] G.M.Bilei,[31] R.Bizzarri,[34] J.J.Blaising,[4] G.J.Bobbink,[15,2] M.Bocciolini,[14] R.Bock,[1] A.Böhm,[1] B.Borgia,[34] M.Boseti,[24] D.Bourilkov,[28] M.Bourquin,[17] D.Boutigny,[4] B.Bouwens,[2] E.Brambilla,[26] J.G.Branson,[36] I.C.Brock,[32] M.Brooks,[21] C.Buisson,[22] A.Bujak,[42] J.D.Burger,[13] W.J.Burger,[17] J.Busenitz,[41] X.D.Cai,[16] M.Capell,[20] M.Caria,[31] G.Carlino,[26] F.Carminati,[14] A.M.Cartacci,[14] R.Castello,[24] M.Cerrada,[23] F.Cesaroni,[34] Y.H.Chang,[13] U.K.Chaturvedi,[16] M.Chemarin,[22] A.Chen,[47] C.Chen,[6] G.M.Chen,[6] H.F.Chen,[18] H.S.Chen,[6] J.Chen,[13] M.Chen,[13] M.L.Chen,[3] W.Y.Chen,[16] G.Chiefari,[26] C.Y.Chien,[5] M.Chmeissani,[3] M.T.Choi,[40] S.Chung,[13] C.Civinini,[14] I.Clare,[13] R.Clare,[13] T.E.Coan,[21] H.O.Cohn,[29] G.Coignet,[4] N.Colino,[15] A.Contin,[7] F.Crijns,[28] X.T.Cui,[16] X.Y.Cui,[16] T.S.Dai,[13] R.D'Alessandro,[14] R.de Asmundis,[26] A.Degré,[4] K.Deiters,[13] E.Dénes,[11] P.Denes,[33] F.DeNotaristefani,[34] M.Dhina,[45] D.DiBitonto,[41] M.Diemoz,[34] H.R.Dimitrov,[39] C.Dionisi,[34,15] M.T.Dova,[16] E.Drago,[26] T.Driever,[28] D.Duchesneau,[17] P.Duinker,[2] I.Duran,[37] S.Easo,[31] H.El Mamouni,[22] A.Engler,[32] F.J.Eppling,[13] F.C.Erné,[2] P.Extermann,[17] R.Fabbretti,[43] M.Fabre,[43] S.Falciano,[34] S.J.Fan,[38] O.Fackler,[20] J.Fay,[22] M.Felcini,[15] T.Ferguson,[32] D.Fernandez,[23] G.Fernandez,[23] F.Ferroni,[34] H.Fesefeldt,[1] E.Fiandrini,[31] J.Field,[17] F.Filthaut,[28] G.Finocchiaro,[34] P.H.Fisher,[5] G.Forconi,[17] T.Foreman,[2] K.Freudenreich,[45] W.Friebel,[44] M.Fukushima,[13] M.Gailloud,[19] Yu.Galaktionov,[25,13] E.Gallo,[14] S.N.Ganguli,[15,8] P.Garcia-Abia,[23] S.S.Gau,[47] D.Gele,[22] S.Gentile,[34,15] S.Goldfarb,[10] Z.F.Gong,[18] E.Gonzalez,[23] P.Göttlicher,[1] A.Gougas,[5] D.Goujon,[17] G.Gratta,[30] C.Grinnell,[13] M.Gruenewald,[30] C.Gu,[16] M.Guanziroli,[16] J.K.Guo,[38] V.K.Gupta,[33] A.Gurtu,[8] H.R.Gustafson,[3] L.J.Gutay,[42] K.Hangarter,[1] A.Hasan,[16] D.Hauschildt,[2] C.F.He,[38] T.Hebbeker,[1] M.Hebert,[36] U.Herten,[1] A.Hervé,[15] K.Hilgers,[1] H.Hofer,[45] H.Hoorani,[17] G.Hu,[16] G.Q.Hu,[38] B.Ille,[22] M.M.Ilyas,[16] V.Innocente,[15] H.Janssen,[15] S. Jezequel,[4] B.N.Jin,[6] L.W.Jones,[3] A.Kasser,[19] R.A.Khan,[16] Yu.Kamyshkov,[29] P.Kapinos,[35,44] J.S.Kapustinsky,[21] Y.Karyotakis,[15] M.Kaur,[16] S.Khokhar,[16] M.N.Kienzle-Focacci,[17] J.K.Kim,[40] S.C.Kim,[40] Y.G.Kim,[40] W.W.Kinnison,[21] D.Kirkby,[30] S.Kirsch,[44] W.Kittel,[28] A.Klimentov,[13,25] A.C.König,[28] E.Koffeman,[2] O.Kornadt,[1] V.Koutsenko,[13,25] A.Koulbardis,[35] R.W.Kraemer,[32] T.Kramer,[13] V.R.Krastev,[39,31] W.Krenz,[1] A.Krivshich,[35] H.Kuijten,[28] K.S.Kumar,[12] A.Kunin,[12,25] G.Landi,[14] D.Lanske,[1] S.Lanzano,[26] P.Lebrun,[22] P.Lecomte,[45] P.Lecoq,[15] P.Le Coultre,[45] D.M.Lee,[21] I.Leedom,[10] J.M.Le Goff,[15] R.Leiste,[44] M.Lenti,[14] E.Leonardi,[34] J.Lettry,[45] X.Leytens,[2] C.Li,[18,16] H.T.Li,[6] P.J.Li,[38] X.G.Li,[6] J.Y.Liao,[38] W.T.Lin,[47] Z.Y.Lin,[18] F.L.Linde,[15] B.Lindemann,[1] D.Linnhofer,[45] L.Lista,[26] Y.Liu,[16] W.Lohmann,[44,15] E.Longo,[34] Y.S.Lu,[6] J.M.Lubbers,[15] K.Lübelsmeyer,[1] C.Luci,[34] D.Luckey,[7,13] L.Ludovici,[34] L.Luminari,[34] W.Lustermann,[44] J.M.Ma,[6] W.G.Ma,[18] M.MacDermott,[45] P.K.Malhotra,[8]† R.Malik,[16] A.Malinin,[4,25] C.Maña,[23] D.N.Mao,[3] Y.F.Mao,[6] M.Maolinbay,[45] P.Marchesini,[45] F.Marion,[4] A.Marin,[9] J.P.Martin,[22] L.Martinez-Laso,[23] F.Marzano,[34] G.G.G.Massaro,[2] T.Matsuda,[13] K.Mazumdar,[8] P.McBride,[12] T.McMahon,[42] D.McNally,[45] M.Merk,[28] L.Merola,[26] M.Meschini,[14] W.J.Metzger,[28] Y.Mi,[19] G.B.Mills,[21] Y.Mir,[16] G.Mirabelli,[34] J.Mnich,[1] M.Möller,[1] B.Monteleoni,[14] R.Morand,[4] S.Morganti,[34] N.E.Moulai,[16] R.Mount,[30] S.Müller,[1] A.Nadtochy,[35] E.Nagy,[11] M.Napolitano,[26] F.Nessi-Tedaldi,[45] H.Newman,[30] C.Neyer,[45] M.A.Niaz,[16] A.Nippe,[1] H.Nowak,[44] G.Organtini,[34] D.Pandoulas,[1] S.Paoletti,[14] P.Paolucci,[26] G.Passaleva,[14,31] S.Patricelli,[26] T.Paul,[5] M.Pauluzzi,[31] F.Pauss,[45] Y.J.Pei,[1] S.Pensotti,[24] D.Perret-Gallix,[4] J.Perrier,[17] A.Pevsner,[5] D.Piccolo,[26] M.Pieri,[15] P.A.Piroué,[33] F.Plasil,[29] V.Plyaskin,[25] M.Pohl,[45] V.Pojidaev,[25,14] N.Produit,[17] J.M.Qian,[3] K.N.Qureshi,[16] R.Raghavan,[8] G.Rahal-Callot,[45] P.G.Rancoita,[24] M.Rattaggi,[24] G.Raven,[2] P.Razis,[27] K.Read,[29] D.Ren,[45] Z.Ren,[16] M.Rescigno,[34] S.Reucroft,[10] A.Ricker,[1] S.Riemann,[44] W.Riemers,[42] K.Riles,[3] O.Rind,[3] H.A.Rizvi,[16] F.J.Rodriguez,[23] B.P.Roe,[3] M.Röhner,[1] S.Röhner,[1] L.Romero,[23] J.Rose,[1] S.Rosier-Lees,[4] R.Rosmalen,[28] Ph.Rosselet,[19] A.Rubbia,[13] J.A.Rubio,[15] H.Rykaczewski,[45] M.Sachwitz,[44] J.Salicio,[15] J.M.Salicio,[23] G.S.Sanders,[21] A.Santocchia,[31] M.S.Sarakinos,[13] G.Sartorelli,[7,16] M.Sassowsky,[1] G.Sauvage,[4] V.Schegelsky,[35] D.Schmitz,[1] P.Schmitz,[1] M.Schneegans,[4] N.Scholz,[45] H.Schopper,[46] D.J.Schotanus,[28] H.J.Schreiber,[44] R.Schulte,[1] S.Schulte,[1] K.Schultze,[1] J.Schwenke,[1] G.Schwering,[1] C.Sciacca,[26] I.Scott,[12] R.Sehgal,[16] P.G.Seiler,[43] J.C.Sens,[15,2] L.Servoli,[31] I.Sheer,[36] D.Z.Shen,[38] S.Shevchenko,[30] X.R.Shi,[30] S.Shotkin,[13] J.Shukla,[32] E.Shumilov,[25] V.Shoutko,[25] E.Soderstrom,[33] D.Son,[40] A.Sopczak,[36] C.Spartiotis,[5] T.Spickermann,[1] P.Spillantini,[14] R.Starosta,[1] M.Steuer,[7,13] D.P.Stickland,[33] F.Sticozzi,[13] H.Stone,[17] K.Strauch,[12] B.C.Stringfellow,[42] K.Sudhakar,[8] G.Sultanov,[16] R.L.Sumner,[33] L.Z.Sun,[18,16] H.Suter,[45] R.B.Sutton,[32] J.D.Swain,[16] A.A.Syed,[16] X.W.Tang,[6] L.Taylor,[10] G.Terzi,[24] C.Timmermans,[28] Samuel C.C.Ting,[13] S.M.Ting,[13] M.Tonutti,[1] S.C.Tonwar,[8] J.Tóth,[11] A.Tsaregorodtsev,[35] G.Tsipolitis,[32] C.Tully,[30] K.L.Tung,[6] J.Ulbricht,[45] L.Urbán,[11] U.Uwer,[1] E.Valente,[34] R.T.Van de Walle,[28] I.Vetlitsky,[25] G.Viertel,[45] P.Vikas,[16] U.Vikas,[16] M.Vivargent,[4] H.Vogel,[32] H.Vogt,[44] I.Vorobiev,[25] A.A.Vorobyov,[35] L.Vuilleumier,[19] M.Wadhwa,[16] W.Wallraff,[1] C.R.Wang,[18] G.H.Wang,[32] J.H.Wang,[6] X.L.Wang,[18] Y.F.Wang,[13] Z.M.Wang,[16,18] A.Weber,[1] J.Weber,[45] R.Weill,[19] T.J.Wenaus,[20] J.Wenninger,[17] M.White,[13] C.Willmott,[23] F.Wittgenstein,[15] D.Wright,[33] R.J.Wu,[6] S.X.Wu,[16] Y.G.Wu,[6] B.Wysłouch,[13] Y.Y.Xie,[38] Y.D.Xu,[6] Z.Z.Xu,[18] Z.L.Xue,[38] D.S.Yan,[38] X.J.Yan,[13] B.Z.Yang,[18] C.G.Yang,[6] G.Yang,[16] K.S.Yang,[6] Q.Y.Yang,[6] Z.Q.Yang,[38] C.H.Ye,[16] J.B.Ye,[18] Q.Ye,[16] S.C.Yeh,[47] Z.W.Yin,[38] J.M.You,[16] N.Yunus,[16] M.Yzerman,[2] C.Zaccardelli,[30] P.Zemp,[45] M.Zeng,[16] Y.Zeng,[1] D.H.Zhang,[2] Z.P.Zhang,[18,16] B.Zhou,[9] J.F.Zhou,[1] R.Y.Zhu,[30] H.L.Zhuang,[6] A.Zichichi,[7,15,16] B.C.C.van der Zwaan.[2]

1 I. Physikalisches Institut, RWTH, W-5100 Aachen, FRG[§]
III. Physikalisches Institut, RWTH, W-5100 Aachen, FRG[§]
2 National Institute for High Energy Physics, NIKHEF, NL-1009 DB Amsterdam, The Netherlands
3 University of Michigan, Ann Arbor, MI 48109, USA
4 Laboratoire d'Annecy-le-Vieux de Physique des Particules, LAPP,IN2P3-CNRS, BP 110, F-74941 Annecy-le-Vieux CEDEX, France
5 Johns Hopkins University, Baltimore, MD 21218, USA
6 Institute of High Energy Physics, IHEP, Beijing, China
7 INFN-Sezione di Bologna, I-40126 Bologna, Italy
8 Tata Institute of Fundamental Research, Bombay 400 005, India
9 Boston University, Boston, MA 02215, USA
10 Northeastern University, Boston, MA 02115, USA
11 Central Research Institute for Physics of the Hungarian Academy of Sciences, H-1525 Budapest 114, Hungary[‡]
12 Harvard University, Cambridge, MA 02139, USA
13 Massachusetts Institute of Technology, Cambridge, MA 02139, USA
14 INFN Sezione di Firenze and University of Florence, I-50125 Florence, Italy
15 European Laboratory for Particle Physics, CERN, CH-1211 Geneva 23, Switzerland
16 World Laboratory, FBLJA Project, CH-1211 Geneva 23, Switzerland
17 University of Geneva, CH-1211 Geneva 4, Switzerland
18 Chinese University of Science and Technology, USTC, Hefei, Anhui 230 029, China
19 University of Lausanne, CH-1015 Lausanne, Switzerland
20 Lawrence Livermore National Laboratory, Livermore, CA 94550, USA
21 Los Alamos National Laboratory, Los Alamos, NM 87544, USA
22 Institut de Physique Nucléaire de Lyon, IN2P3-CNRS,Université Claude Bernard, F-69622 Villeurbanne Cedex, France
23 Centro de Investigaciones Energeticas, Medioambientales y Tecnologicas, CIEMAT, E-28040 Madrid, Spain
24 INFN-Sezione di Milano, I-20133 Milan, Italy
25 Institute of Theoretical and Experimental Physics, ITEP, Moscow, Russia
26 INFN-Sezione di Napoli and University of Naples, I-80125 Naples, Italy
27 Department of Natural Sciences, University of Cyprus, Nicosia, Cyprus
28 University of Nymegen and NIKHEF, NL-6525 ED Nymegen, The Netherlands
29 Oak Ridge National Laboratory, Oak Ridge, TN 37831, USA
30 California Institute of Technology, Pasadena, CA 91125, USA
31 INFN-Sezione di Perugia and Universitá Degli Studi di Perugia, I-06100 Perugia, Italy
32 Carnegie Mellon University, Pittsburgh, PA 15213, USA
33 Princeton University, Princeton, NJ 08544, USA
34 INFN-Sezione di Roma and University of Rome, "La Sapienza", I-00185 Rome, Italy
35 Nuclear Physics Institute, St. Petersburg, Russia
36 University of California, San Diego, CA 92182, USA
37 Dept. de Fisica de Particulas Elementales, Univ. de Santiago, E-15706 Santiago de Compostela, Spain
38 Shanghai Institute of Ceramics, SIC, Shanghai, China
39 Bulgarian Academy of Sciences, Institute of Mechatronics, BU-1113 Sofia, Bulgaria
40 Center for High Energy Physics, Korea Advanced Inst. of Sciences and Technology, 305-701 Taejon, Republic of Korea
41 University of Alabama, Tuscaloosa, AL 35486, USA
42 Purdue University, West Lafayette, IN 47907, USA
43 Paul Scherrer Institut, PSI, CH-5232 Villigen, Switzerland
44 DESY-Institut für Hochenergiephysik, O-1615 Zeuthen, FRG
45 Eidgenössische Technische Hochschule, ETH Zürich, CH-8093 Zürich, Switzerland
46 University of Hamburg, W-2000 Hamburg, FRG
47 High Energy Physics Group, Taiwan, China
§ Supported by the German Bundesministerium für Forschung und Technologie
‡ Supported by the Hungarian OTKA fund under contract number 2970.
† Deceased.

References

[1] A.D. Dolgov, L.B. Okun and V.I. Zakharov, Nucl. Phys. B41 (1972) 197;
E. Ma and J. Okada, Phys. Rev. Lett. 41 (1978) 287;
K.J. Gaemers, R. Gastmans and F.M. Renard, Phys. Rev. D19 (1979) 1605;
G. Barbiellini, B. Richter and J. Siegrist, Phys. Lett. B 106 (1981) 414.

[2] L3 Collaboration, O. Adriani *et al.*, CERN preprint CERN PPE/92–128;
L3 Collaboration, B. Adeva *et al.*, Phys. Lett. B275 (1992) 209;
OPAL Collaboration, M.Z. Akrawy *et al.*, Z. Phys. C50 (1991) 373.

[3] M. Chen, C. Dionisi, M. Martinez and X .Tata, Phys. Rep. C 159, (1988) 203;
R. Barbieri *et al.*, CERN-EP/89-08, Vol. 2, (1989) 121.

[4] F. Boudjema and A. Djouadi, Phys. Lett. B 240 (1990) 485.

[5] F.M. Renard, Nucl. Phys. B196 (1982) 93;
A. Barroso, F. Boudjema, J. Cole, and N. Dombey, Z. Phys. C28 (1985) 149.

[6] Duane A. Dicus, S. Nandi, and Jeffrey Woodside, Phys. Lett. B 258 (1991) 231.

[7] J.E. Kim and U.W. Lee, Phys. Lett. B 233 (1989) 496.

[8] L3 Collaboration, B. Adeva *et al.*, Phys. Lett. B 252 (1990) 525;
L3 Collaboration, B. Adeva *et al.*, to be published in Physics Reports.

[9] L3 Collaboration, B. Adeva *et al*, Nucl. Inst. Meth. A289 (1990) 35.

[10] R. Brun *et al.*, GEANT3 Users Guide, CERN/DD/EE/84.1.

[11] H. Fesefeldt, RWTH Aachen Report PITHA 85/02 (1985).

[12] R. Bizzarri *et al.*, Nucl. Inst. Meth. A317 (1992) 463.

[13] L3 Collaboration, O. Adriani *et al.*, CERN preprint CERN PPE/92–128.

[14] A. Barroso, P. Nogueira, J.C. Romao, Phys. Lett. 196B (1987) 547.

[15] F. Boudjema, Phys. Rev. D36 (1987) 969;
F. Boudjema and N. Dombey, Z. Phys. C35 (1987) 499.

[16] M. Baillargeon and F. Boudjema, CERN Report 92-04, p. 178.

[17] John F. Gunion and Howard E. Haber, Nucl. Phys. B272 (1986) 1.

Figure Captions

Figure 1 Single–photon energy distributions for data (points) and Monte Carlo (histograms) summed over all center–of-mass energies. Cross–hatched histogram is from $e^+e^- \rightarrow \nu\bar{\nu}\gamma$ according to the Standard Model with three neutrino families, sum of the cross-hatched and open histograms represents expectation for $e^+e^- \rightarrow \nu\bar{\nu}\gamma$ with $\beta = 1$, and shaded histogram is expected distribution from the QED background processes $e^+e^- \rightarrow e^+e^-\gamma$ and $e^+e^- \rightarrow \gamma\gamma\gamma$.

Figure 2 Single–photon energy distributions for data (points) and Monte Carlo (histograms) at $\sqrt{s}$ = 91.25 GeV. Cross–hatched histogram is from $e^+e^- \rightarrow \nu\bar{\nu}\gamma$ according to the Standard Model with three neutrino families, open histogram is expectation for $e^+e^- \rightarrow \tilde{G}\tilde{G}\gamma$ with $\mu = -100$ GeV, $\tan\beta = 2$, M = 30 GeV, and $m_{\tilde{G}}=3 \times 10^{-14}$ GeV, and shaded histogram is expected distribution from the QED background processes $e^+e^- \rightarrow e^+e^-\gamma$ and $e^+e^- \rightarrow \gamma\gamma\gamma$.

Figure 3 (a) Lower limits (95% C.L.) on gravitino mass as a function μ for $\tan\beta$=1 and several different values of M. The numerical label for each curve is M in units of GeV. (b) Same as (a) except $\tan\beta$=10

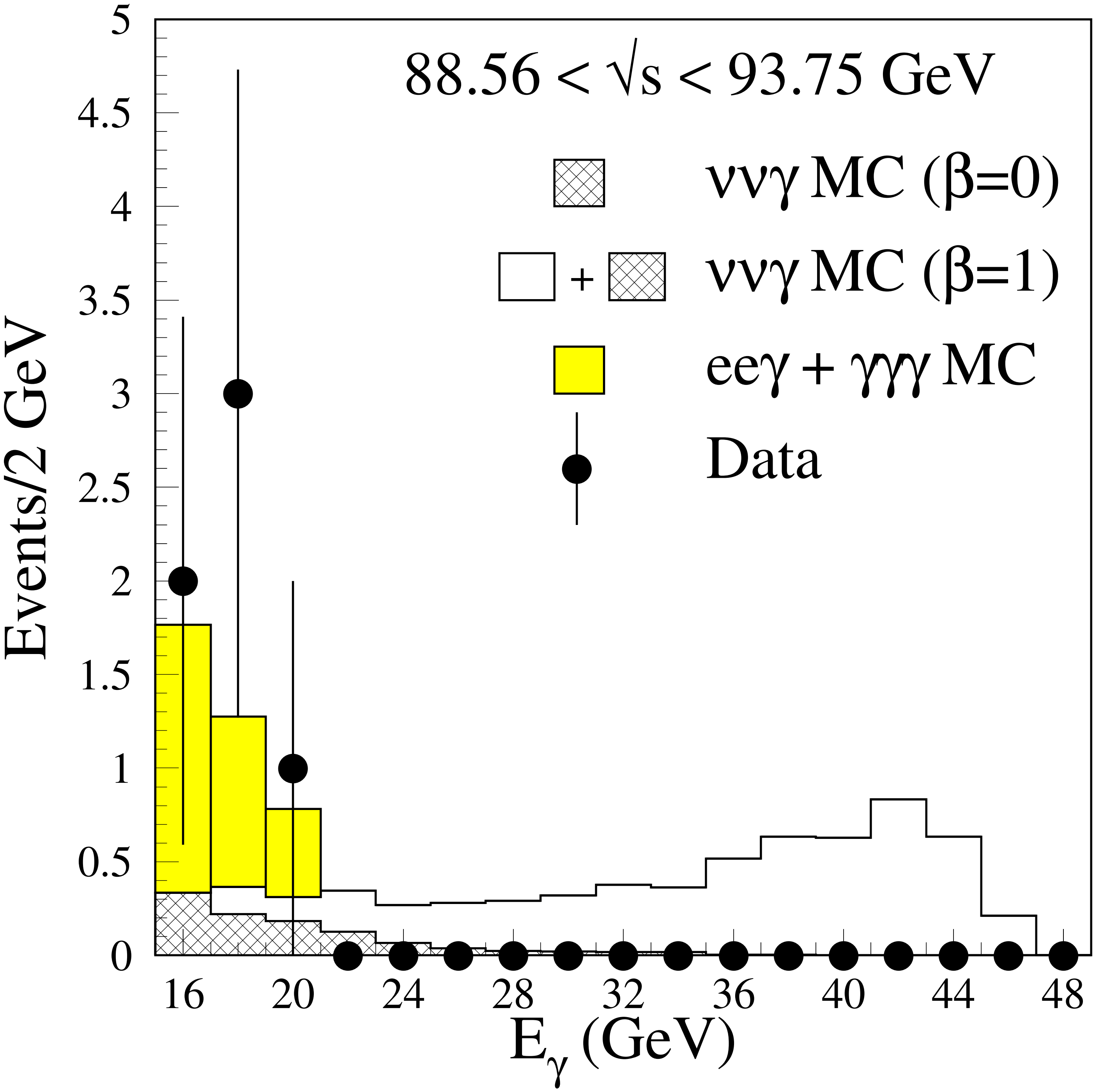

88.56 < √s < 93.75 GeV
ννγ MC (β=0)
+ ννγ MC (β=1)
eeγ + γγγ MC
Data
Events/2 GeV
E_γ (GeV)
0
0.5
1
1.5
2
2.5
3
3.5
4
4.5
5
16
20
24
28
32
36
40
44
48

Figure 1

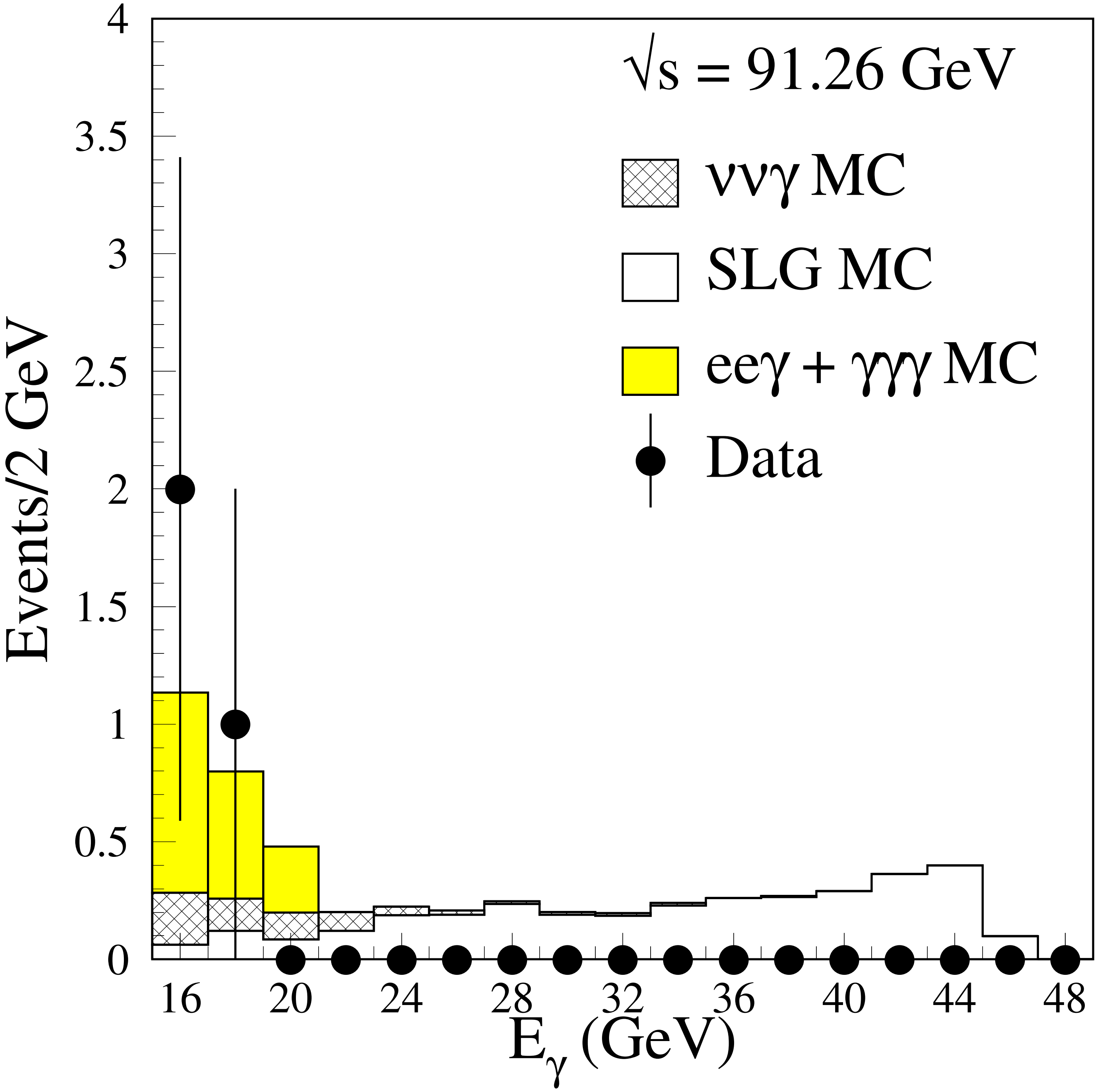

√s = 91.26 GeV
ννγ MC
SLG MC
eeγ + γγγ MC
Data
Events/2 GeV
4
3.5
3
2.5
2
1.5
1
0.5
0
16
20
24
28
32
36
40
44
48
E$_\gamma$ (GeV)

Figure 2